Available online at www.sciencedirect.com
SCIENCE DIRECT®
Journal of Catalysis 224 (2004) 252–260
JOURNAL OF CATALYSIS
www.elsevier.com/locate/jcat

A combined transient and computational study of the dissociation of N_2O on platinum catalysts

R. Burch,* S.T. Daniells,[1] J.P. Breen, and P. Hu

CenTACat, School of Chemistry, David Keir Building, Stranmillis Road, Queen's University Belfast, Belfast, Northern Ireland BT9 5AG, UK

Received 20 November 2003; revised 5 March 2004; accepted 5 March 2004

Available online 16 April 2004

Abstract

The energetics of the low-temperature adsorption and decomposition of nitrous oxide, N_2O, on flat and stepped platinum surfaces were calculated using density-functional theory (DFT). The results show that the preferred adsorption site for N_2O is an atop site, bound upright via the terminal nitrogen. The molecule is only weakly chemisorbed to the platinum surface. The decomposition barriers on flat (111) surfaces and stepped (211) surfaces are similar. While the barrier for N_2O dissociation is relatively small, the surface rapidly becomes poisoned by adsorbed oxygen. These findings are supported by experimental results of pulsed N_2O decomposition with 5% Pt/SiO_2 and bismuth-modified Pt/C catalysts. At low temperature, decomposition occurs but self-poisoning by $O_{(ads)}$ prevents further decomposition. At higher temperatures some desorption of O_2 is observed, allowing continued catalytic activity. The study with bismuth-modified Pt/C catalysts showed that, although the activation barriers calculated for both terraces and steps were similar, the actual *rate* was different for the two surfaces. Steps were found experimentally to be more active than terraces and this is attributed to differences in the preexponential term.

Keywords: DFT; N_2O decomposition; Platinum; Catalysis

1. Introduction

The ever increasingly stringent legislation aimed at reducing the emission of NO_x (defined as NO and NO_2) from mobile and stationary power sources has provided a focus for catalysis research for 4 decades. The success of the three-way catalytic converter is founded on operating temperatures above 200 °C and an exhaust gas with a composition close to stoichiometric [1]. However, with engine operation under lean-burn conditions or at low temperatures, three-way catalysts are incapable of removing all the NO_x [2,3]. In addition, the exhaust temperatures and conditions of diesel engines and high efficiency gas boilers are often <150 °C. Under these conditions, significant quantities of NO_x are converted to N_2O instead of N_2, and no onboard technology is currently employed to remove this pollutant.

N_2O is a potent greenhouse gas, exhibiting approximately 300 times the greenhouse activity of CO_2 (over a 100 year span on a weight basis) [4–6], and also contributes to stratospheric ozone depletion [7]. Many catalytic systems have been employed for N_2O decomposition, including metals, pure and mixed oxides, supported metals, and zeolites [7]. A general mechanism was proposed by Winter in the late 1960s [8–10].

$$N_2O + * \rightarrow N_2 + O^*, \quad (1)$$

$$2O^* \leftrightarrow O_2 + 2^*, \quad (2)$$

$$N_2O + O^* \rightarrow N_2 + O_2. \quad (3)$$

Weinberg [11] concluded that Pt would exhibit poor activity for N_2O decomposition based on bond energy bond order (BEBO) calculations used together with absolute rate theory. The N–N bond is significantly stronger (474.163 kJ mol^{-1}) than the N–O bond (161.38 kJ mol^{-1}) and therefore one would expect catalytic decomposition yielding $N_2 + O$ to be energetically favored. Weinberg [11] also claims, under his experimental conditions of 1125 K and $pN_2O \sim 10^{-8}$ Torr, that a Pt surface would only dissociate ∼ 0.5% of the impinging molecules, and that the

* Corresponding author.
E-mail address: R.Burch@qub.ac.uk (R. Burch).
[1] Present address: DelftChemTech, Reactor and Catalysis Engineering, Faculty of Applied Sciences, Delft University of Technology, Julianalaan, 136, 2628 BL Delft, The Netherlands.

0021-9517/$ – see front matter
doi:10.1016/j.jcat.2004.03.027

surface would remain virtually clean throughout the whole reaction. Taking into account these kinetic considerations, Avery [12] studied N_2O decomposition on a Pt(111) surface using electron energy loss spectra (EELS). After dosing N_2O onto the surface, a weak band at 325 cm^{-1} was assigned to the υ(Pt–N_2O) mode. However, after desorption at 105 K no characteristic υ(Pt–O) band at 470 cm^{-1} was observed for any residual oxygen, thereby suggesting that no decomposition of N_2O occurred [12].

However, Takoudis and Schmidt [13], and Lintz and Riekert [14], using a Pt wire filament and ribbon, respectively, reported significant activity toward N_2O decomposition. The latter reported that N_2O was observed to decompose even at room temperature to give $N_{2(g)}$ and chemisorbed oxygen [14]. Indeed, Takoudis and Schmidt reported unity coverage of N_2O at low temperature, and a coverage proportional to the partial pressure of N_2O at higher pressures [13]. At low N_2O partial pressure, Takoudis and Schmidt determined an activation energy of 146 kJ mol^{-1} at the surface, and a heat of adsorption of 89 kJ mol^{-1} [13]. In addition, they concluded that N_2O decomposition on polycrystalline Pt was 50–100 times faster than NO dissociation at temperatures greater than 550 °C.

Dissociative adsorption of N_2O on supported Pt was studied by Kim et al. [15] who claimed that, regardless of the conclusions drawn from UHV studies for N_2O on platinum, their experiments showed decomposition of N_2O on Pt at 363 K and 76 Torr yielding $N_{2(g)}$ and an $O_{(ads)}$ monolayer. Denton et al. [16], using N_2O pulse experiments with 0.9% Pt/SiO_2 at 220 °C, showed that N_2O decomposition does occur, producing N_2 and adsorbed oxygen (TPD experiments show that O_2 does not desorb from platinum below 500 °C [17]). As the surface concentration of oxygen increases the activity decreases. No decomposition of nitrous oxide is observed on a completely oxidized surface [16]. Therefore, Eqs. (2) and (3), which involve removal of strongly adsorbed oxygen, would not be expected to occur at low temperatures.

An added importance of studying the formation and decomposition of N_2O is the consideration that it could be an intermediate in N_2 formation during selective catalytic reduction (SCR) of NO_x. The decomposition rate of N_2O adsorbed directly from the gas phase, particularly on Pt, is at a level that suggests little or no participation in the formation of N_2 [18–20]. On the other hand, preadsorbed N_2O could be an intermediate species in N_2 formation. However, Cho [21–23] in his analysis of the NO + CO reaction states that N_2O can continuously adsorb and desorb via an exchange process, and hence no distinction between $N_2O_{(g)}$ and $N_2O_{(ads)}$ can be made.

There is a significant debate in the literature as to the possible role of an N_2O intermediate in N_2 formation as part of an overall deNO_x reaction, and also with regard to the actual mechanism of formation of N_2 and N_2O. Ohno et al. [24,25], using LEED-AES and AR-TDS on Pd(110), reported that the angular and velocity distributions of desorbing N_2 produced by independent NO and N_2O decomposition reactions are so similar that this suggests that $N_2O_{(ads)}$ is an intermediate in N_2 formation. Denton and co-workers [16] performed pulsed NO and N_2O decomposition experiments with Pt/SiO_2. For the NO experiments, N_2O, NO, and N_2 were all observed, while, for N_2O decomposition, only N_2 and unreacted N_2O were present. This led them to propose that any NO → N_2O conversions are irreversible, and therefore both N_2 and N_2O are formed from NO dissociation [16].

One possible explanation to the disagreements in the literature has been provided by Burch and co-workers [26–31] based on steady-state isotopic transient kinetic analysis (SSITKA) of NO reduction reactions. After mathematical modeling of their results, they proposed the existence of a "pseudo-adsorbed" N_2O species that, while chemically equivalent, is electronically different to N_2O. This work goes further by concluding that N_2O is formed from two identical surface species ($NO_{(ads)} + NO_{(ads)}$ being the most plausible), whereas N_2 is formed from different surface species (for example, $NO_{(ads)} + N_{(ads)}$). The existence of an $(NO)_2$ dimer species for N_2O formation has been suggested by others. Using transient techniques to study NO and N_2O decomposition on Rh catalysts, Rahkamaa and Salmi [32] proposed a mechanism involving an (*ON...NO^*) species, in agreement with Burch et al. However, their mechanism goes on to suggest that N_2 is also formed via the same intermediate species, and that some N_2 is a product of the self-decomposition of $N_2O_{(ads)}$.

In this paper we report the results from density-functional theory calculations of N_2O decomposition, $N_2O \rightarrow N_2O_{(ads)} \rightarrow N_2 + O_{(ads)}$, on flat Pt(111) and stepped Pt(211) surfaces. The transition-state geometries assumed and activation barriers are reported for the first time. The results from a complementary experimental study are also included and compared with the predictions of the DFT calculations.

2. Experimental and calculation details

A sample of 5% Pt/SiO_2 was prepared by incipient wetness impregnation using Pt-DNDA (Johnson Matthey) precursor and acid-washed silica (Grace 432) with mesh range 250–850 μm. After impregnation, the catalyst was dried at 120 °C overnight prior to calcination at 500 °C for 2 h. One hundred-milligram test samples were positioned in a Pyrex tube and held in place between two quartz wool plugs. A thermocouple was positioned in the catalyst bed to monitor temperature and the reactor furnace was controlled using a Eurotherm 818 controller. The reactant gases, He (100%, BOC Gases), N_2O (0.2% in He, BOC Gases), and H_2 (3% in He, BOC Gases) were fed from independent Aera mass-flow controllers. Reaction products were monitored using a computer interfaced Fisons Gaslab 300 mass spectrometer, operated using the corresponding Thermosoft software. Prior to testing, all samples were pretreated in 1% H_2/He, total flow rate = 50 $cm^3\,min^{-1}$, for 30 min at 500 °C. The

size of the sample loop was designed to titrate 10% of the surface per pulse, assuming 1:1 N_2O:Pt.

Steady-state experiments were monitored using a PC interfaced Perkin-Elmer Autosystem XL GC fitted with a 13X molecular sieve column. One hundred-milligram samples were held between two quartz wool plugs in a quartz reactor. The sample was pretreated with 1% H_2/He, total flow rate = 200 $cm^3\,min^{-1}$, for 30 min at 500 °C.

The 5% Pt/C catalyst was obtained from Johnson Matthey and used without further modification. Surface modification by bismuth was achieved by irreversible adsorption of aqueous bismuth ions from a 7.2×10^{-4} M solution of bismuth nitrate. One gram of catalyst was stirred with 7 or 15 cm^3 of the bismuth solution for several hours followed by rinsing with pure water and drying at 80 °C for 12 h [33]. The coverage of the Pt surface by Bi is measured in monolayers (ML).

All calculations were carried out within the DFT framework [34–36]. The generalized gradient approximation (GGA) was used for the exchange and correlation functional [37]. Ionic cores were described by ultrasoft pseudopotentials [38] and the Kohn–Sham one-electron states were expanded in a plane-wave basis set up to a cutoff energy of 340 eV. The Pt(111) and Pt(211) surfaces were modeled using periodic three-layer slabs with a p(2 × 2) unit cell and a p(2×3) unit cell, respectively. Both surfaces were modeled with an associated vacuum region of ∼10 Å. Monkhorst–Pack meshes with 3 × 3 × 1 k-grid sampling in the surface Brillouin zone was used. The adsorbates were allowed to relax, while Pt atoms were fixed at their bulk-truncated positions.

Transition states were searched using a constrained optimization scheme [39–42]. For $N_2O \rightarrow N_2 + O_{(ads)}$, the N_{cent}–O bond distance was fixed at a preselected value and minimized with respect to the remaining degrees of freedom (where N_{cent} refers to the central nitrogen in N–N–O; this notation will be used throughout). The transition state (TS) is confirmed when (i) all forces on the atoms disappear, and (ii) the total energy is a maximum with respect to the reaction coordinate and a minimum with respect to all remaining degrees of freedom [39–41].

3. Results and discussion

3.1. DFT calculations of the molecular adsorption of N_2O on Pt(111)

Nitrous oxide adsorption on metal surfaces has been reported and discussed elsewhere in the literature [11,12,14, 15,42]. However, there existed some debate as to the orientation of the N_2O molecule on the surface with some authors proposing adsorption via the oxygen and some suggesting adsorption via the terminal nitrogen atom [43]. Geometry optimization calculations were performed for three possible adsorption modes: upright via the terminal N atom, upright via the O atom, and N_2O parallel to the surface. For the latter two cases no chemisorption with the Pt surface was observed. Only via the terminal N, in an upright configuration, will N_2O adsorb on Pt, thereby supporting the conclusions of Li and Bowker [43].

Table 1
Geometric results for N_2O chemisorption on Pt(111)

Adsorption site	$r_{N–O}$ (Å)	$r_{N–N}$	$r_{N–Pt}$	E_{chem}
Atop	1.20	1.14	1.98	0.163
fcc hollow	1.20	1.16	2.38	−0.310
hcp hollow	1.20	1.16	2.41	−0.317
Bridge	1.20	1.16	2.22	−0.166

Notes. $r_{N–O}$ denotes the nitrogen–oxygen bond distance, $r_{N–Pt}$ denotes the nitrogen–platinum bond distance, $r_{N–N}$ denotes the nitrogen–nitrogen bond distance, E_{chem} denotes the chemisorption energy.

Gas phase N_2O is linear with N–N and N–O bond distances of 1.13 and 1.19 Å, respectively. For chemisorption through the N atom the N–Pt bond distance is 1.98 Å, with N–N bond and N–O bond distances of 1.14 and 1.20 Å, respectively. The molecule remains linear, bonded to the surface in an upright configuration. All important geometric parameters for N_2O chemisorption are detailed in Table 1. The most stable, and therefore the preferred, site for N_2O adsorption is the atop site on a Pt(111) surface. For chemisorption at the two 3-fold hollow sites (fcc and hcp) and at the bridge site, negative chemisorption energies were calculated suggesting a barrier for N_2O adsorption at these sites. However, the chemisorption energy is very small on all the adsorption sites studied, in agreement with the results of Avery [12].

3.2. N_2O dissociation on Pt(111)

Using electron energy loss spectra, Avery [12] reported that no decomposition occurred after dosing N_2O at low temperature onto Pt(111). In the present work N_2O decomposition was modeled using DFT with generalized gradient approximations. The initial state was considered as N_2O in the gas phase and a clean Pt(111) surface. Adsorption was weak, with a chemisorption energy of 0.163 eV. In order to decompose, the molecule must tilt, thereby enabling the oxygen atom to bond with a surface Pt atom. Adsorption to the surface occurs via the terminal N atom on the atop site, followed by tilting of the molecule toward the surface. The structure at the transition state is illustrated in Fig. 1. The terminally bound N atom moves from the atop to an off-atop position, with a N–Pt bond distance at the transition state of 2.02 Å. The O is close to the bridge site at the transition state and the average O–Pt bond distance was 2.3 Å. The molecule is obviously no longer linear, with a decrease from 180 to 120° at the transition state. All the important parameters are detailed in Table 2. It should be noted that the N–O bond distance at the transition state, 1.45 Å, is relatively short, which is different from diatomic molecule dissociations, such as CO [44]. This difference may arise for the following reason: In the diatomic molecule dissociation, both atoms in the TS are on the surface. Therefore, the diatomic molecules

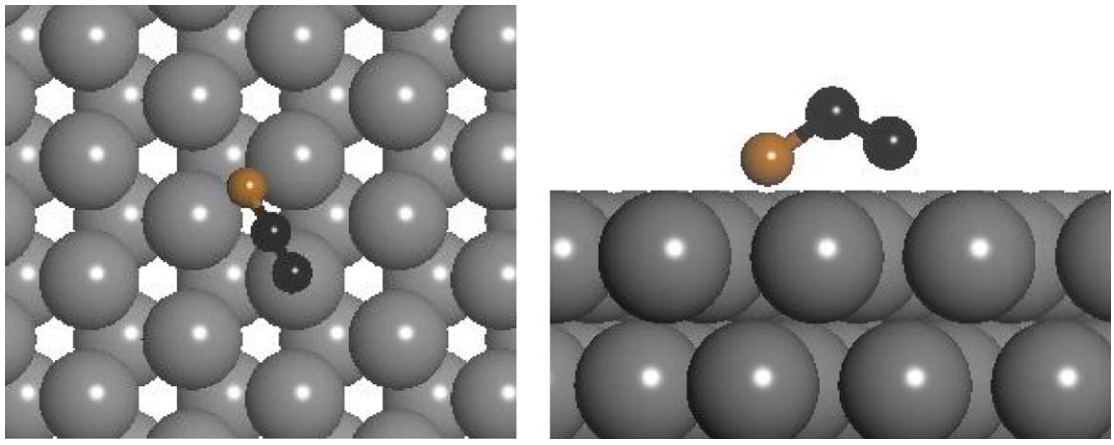

Fig. 1. Transition state of $N_2O \rightarrow N_2O + O_{(ads)}$ on Pt(111). Only two Pt layers are shown for clarity.

Table 2
Geometric parameters for N_2O dissociation on Pt(111) and Pt(211)

N_2O ↓ $N_2 + O_{(ads)}$	$r_{N–O}$ (Å)	$r_{N–N}$ (Å)	$r_{N_{ter}–Pt}$ (Å)	$r_{O–Pt}$ (Å)	N–N–O (deg)
Pt(111)	1.45	1.19	2.02	2.23	120.0
Pt(211)	1.45	1.18	2.07	2.26	137.0

Notes. $r_{N–O}$ denotes the N_{cent}–O bond distance, $r_{N–N}$ denotes the N–N bond distance, $r_{N_{ter}–Pt}$ denotes the N_{ter}–Pt distance, $r_{O–Pt}$ corresponds to the length of the O–Pt bond, and N–N–O denotes the molecular bond angle.

are well stretched in the TS, resulting in the late TS. On the other hand, in N_2O the N that bonds with the O is not directly bonded to any metal atoms, although the O is on the surface in the TS for N_2O dissociation, giving rise to a relatively short NN–O bond at the TS. Once the N_2O molecule bonds with the surface and the O–Pt bond begins to form, decomposition to yield N_2 and $O_{(ads)}$ is facile. The activation energy for this reaction is only 0.32 eV, suggesting that the reaction may occur at low temperatures.

3.3. N_2O dissociation on Pt(211)

Catalyst defect sites have been shown to exhibit significantly higher activity than flat or terrace sites. Nørskov et al. [45] reported an activation energy of 0.14 eV for NO dissociation on a Pt-step surface, while Bogicevic and Hass [46] reported an NO dissociation barrier of 2.10 eV on Pt(111). In the case of NO, the molecule is orientated such that the N atom is at the bottom of the step, while the O atom is chemisorbed at the top of the step. For N_2O dissociation on Pt(211), the oxygen was found from our calculations to be located at the top of the step, as is observed for NO dissociation. In our study a transition state with a low barrier was identified, as shown in Fig. 2. The transition state involves adsorption of the N_2O molecule via both the O atom and the terminal N atom. No bonding occurs between the central N atom and the Pt surface. The terminal N–Pt bond distance is 2.07 Å and the N–N bond distance is 1.18 Å. The O is close to the bridge site and the average O–Pt bond distance

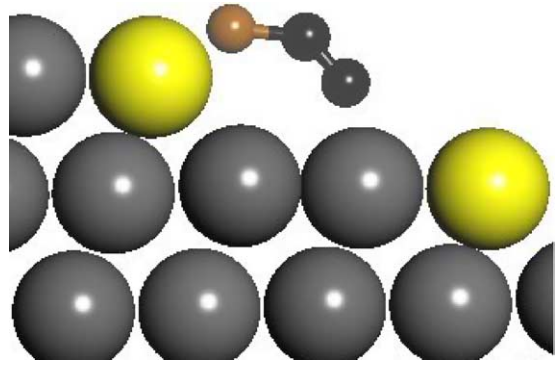

Fig. 2. The possible N_2O dissociation transition state on Pt(211). The large light atoms are the Pt step atoms.

of 2.26 Å. As observed for the transition state on Pt(111), the N–O bond distance at the transition state is 1.45 Å, while the N–N–O bond angle on this surface is 137°. Geometric parameters for the transition state are presented in Table 2.

The activation energy for the reaction $N_2O \rightarrow N_2 + O_{(ads)}$ on Pt(211), 0.44 eV, is similar to that on Pt(111), if N_2O in the gas phase is taken as the initial state. The large differences between the barriers on flat surfaces and the barriers on steps reported for diatomic molecules such as NO and CO are not observed for the triatomic N_2O. Dissociation of NO on a flat (111) surface creates bonding competition for surface Pt atoms because the N and the O have to share bonding with a metal atom at the transition state. This bonding competition [47–49] dramatically increases the activation energy for the process of dissociation. At step sites, the effect of bonding competition is nonexistent as one atom, in the case of NO the N atom, is situated at the base of the step and the other atom, O, is at the top of the step. No atom sharing occurs in this configuration and the barrier for dissociation is considerably lower at step sites.

For N_2O, the dissociation on Pt(111) involves 3 surface Pt atoms, with the N_2O molecule configured with the terminal N atom on the atop position on one Pt atom and the O atom on the bridge site of two separate Pt atoms. No bond-

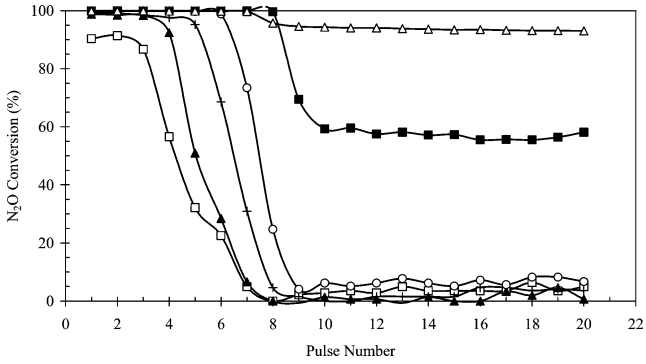

Fig. 3. Conversion of N_2O as a function of pulse number for different temperatures over reduced 5% Pt/SiO_2. Total gas flow = 50 cm^3 min^{-1}, pulses of 2000 ppm N_2O, He balance. 25 °C (□), 150 °C (▲), 250 °C (+), 350 °C (○), 450 °C (■), 500 °C (△).

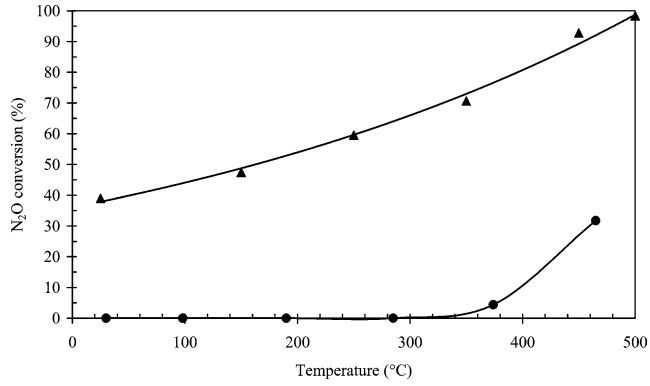

Fig. 4. Total N_2O conversion of pulses 1–10 (▲) over the temperature range 25–500 °C. 1 pulse = 10% surface coverage. Included is the steady-state N_2O conversion over 5% Pt/SiO_2 (●). 2000 ppm N_2O, balance He.

ing competition exists and the barrier of dissociation reflects this, 0.32 eV. The same occurs at the step edge of the Pt surface and the barriers associated with both sites are similar. However, once the site has been occupied with $O_{(ads)}$ no further N_2O decomposition can occur: the $O_{(ads)}$ has poisoned the surface.

3.4. Decomposition of N_2O with real Pt catalysts

The results of pulsing experiments of N_2O decomposition over 5% Pt/SiO_2 are presented in Fig. 3. It can be seen that at 25 °C approximately 90% conversion of N_2O occurs for 3 pulses before activity is rapidly lost. Increasing the temperature enhances the activity and increases the number of pulses that show conversion before catalyst deactivation occurs. At lower temperatures N_2O decomposition yields $N_{2(g)}$ and $O_{(ads)}$, with the latter remaining adsorbed on the surface. At 450 °C, a decrease in the N_2O conversion is observed after 8 pulses but complete deactivation does not occur. Indeed a "steady-state" conversion of ∼ 60% continues well beyond the saturation point of 10 pulses. At 500 °C, this steady-state conversion is approximately 95%.

A 100% titration of the surface with $O_{(ads)}$ was calculated to require 10 pulses of N_2O and the total N_2O conversion recorded for these 10 pulses is displayed in Fig. 4. At 25 °C, approximately 40% of the N_2O is converted to N_2, while at 250 °C conversion has increased to ∼ 60%, and at 500 °C 100% conversion of N_2O is observed. Included in Fig. 4 are the results of actual steady-state conversions of N_2O. From these results it can be seen that Pt/SiO_2 is actually a poor catalyst for direct N_2O decomposition since no significant conversion is observed below 400 °C. The conversions reported here for the pulse experiments show that Pt/SiO_2 is active toward N_2O decomposition but activity is rapidly lost through self-poisoning with $O_{(ads)}$.

TPD experiments by Burch et al. [17] reported no O_2 desorption from oxidized Pt surfaces below 600 °C. However, in our pulse experiments some O_2 desorption was observed at 450 °C. Fig. 5 shows the O_2 desorption profiles for the different temperatures studied, all taken after pulse 15. At this

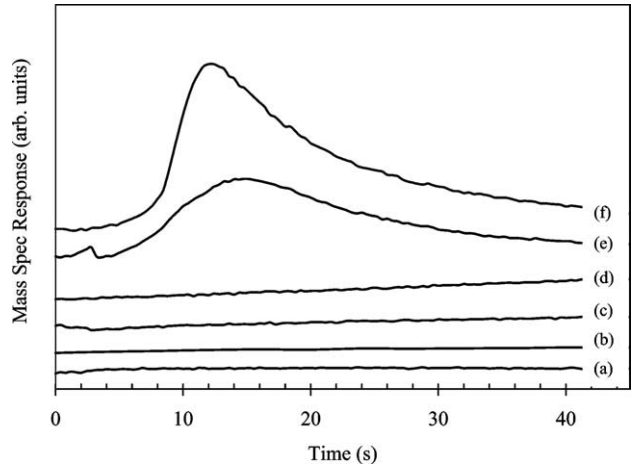

Fig. 5. O_2 desorption profiles during catalytic decomposition of N_2O over 5% Pt/SiO_2 after 15 N_2O pulses. Pulsing 2000 ppm N_2O at 25 °C (a), 150 °C (b), 250 °C (c), 350 °C (d), 450 °C (e), 500 °C (f). $t = 0$ signifies injection of the N_2O pulse.

point the surface is saturated with $O_{(ads)}$ and desorption of O_2 does not commence at 450 or 500 °C until after pulse 10. It is evident from this figure that no O_2 desorption occurs at 25–250 °C. A slight increase in the mass spectrometer response is observed at 350 °C suggesting O_2 desorption from the surface is a slow process. At 450 and 500 °C desorption of O_2 is significant and this recycling of active sites accounts for the continued activity of the catalyst at these temperatures.

The desorption of O_2 from the surface at 450 and 500 °C coincides with a decrease in N_2O conversion to N_2. This is clearly evident in Fig. 6, where a second pulse of N_2O was injected 10 s after the first pulse. O_2 desorption from the surface is delayed relative to N_2 and introduction of a second pulse of N_2O overlaps with the O_2 desorption. N_2O conversion (and N_2 production) decreased in the second pulse. Due to the delayed desorption of O_2 from the surface, access of incoming N_2O molecules to the surface is probably inhibited and therefore N_2O conversion decreases. However, the surface coverage of $O_{(ads)}$ has reached a critical level and

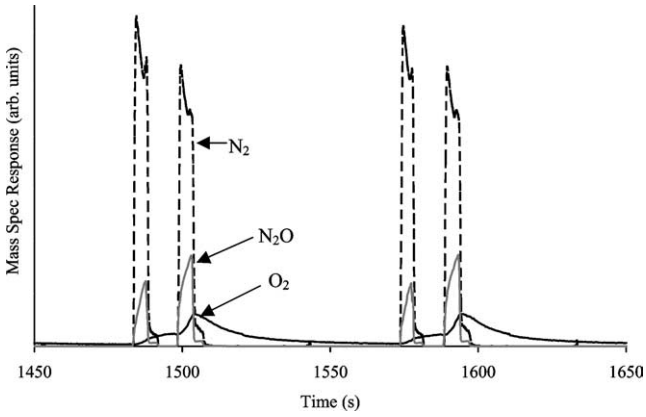

Fig. 6. The effect of introduction of a second N_2O pulse 10 s (pulses 17 and 18) at $T = 450\,^{\circ}C$. 2000 ppm N_2O pulse, balance He.

the kinetic energy of the pulsed N_2O molecules may be sufficient to accelerate some recombination and desorption of O_2 that would otherwise require higher temperatures. This is seen in the small, but significant, increase in the rate of O_2 desorption with the introduction of the second pulse of N_2O. A similar "reaction-assisted" mechanism for O_2 desorption from Rh has been suggested previously by Tanaka et al. [50]. Rahkamaa et al. [32] reported that desorption of molecular oxygen from their Rh surface was less rapid than N_2 liberation during the decomposition reaction. This was due to the stronger adsorption affinity and lower desorption velocity of oxygen.

The delay between observing N_2 and O_2 is evident from studying Eqs. (1) and (2); N_2 is instantly released from the decomposition of N_2O, whereas O_2 formation depends on the recombination of adsorbed surface oxygen atoms. Leglise et al. [51] studied N_2O decomposition over iron-exchanged mordenite, and suggested an N_2O "bombardment" mechanism whereby O_2 is released by a collision with an incoming N_2O molecule in accordance with Eq. (3) [8–10,52,53], freeing a surface redox site: an Eley–Rideal-type mechanism. On the other hand, when the surface was doped with ^{18}O, the expectation being the release of $^{34}O_2$, only $^{32}O_2$ was observed. This suggests that the freed O_2 is produced exclusively from N_2O decomposition on a limited number of surface sites [51]. Clearly, the question of whether or not there is an adsorption-assisted desorption of O_2 in the presence of N_2O is still open.

Carbon-supported platinum catalysts with irreversible, controlled adsorption of inactive Bi were used to probe the catalyst for the active sites for N_2O decomposition. Addition of bismuth preferentially blocked the metal defect sites. Fig. 7 shows cyclic voltammetry data for the unmodified and bismuth surface-modified catalysts. The increase in bismuth loading was signified by a gradual loss in intensity of all peaks in the potential range 0–0.6 V. The cyclic voltammetry, by comparison with results from single crystal samples, showed for the fresh Pt catalyst a predominantly stepped surface ((110)-peak at 0.05 V > (100)-peak at 0.2 V). Although there was some terracing ((100)-broad feature between 0.25

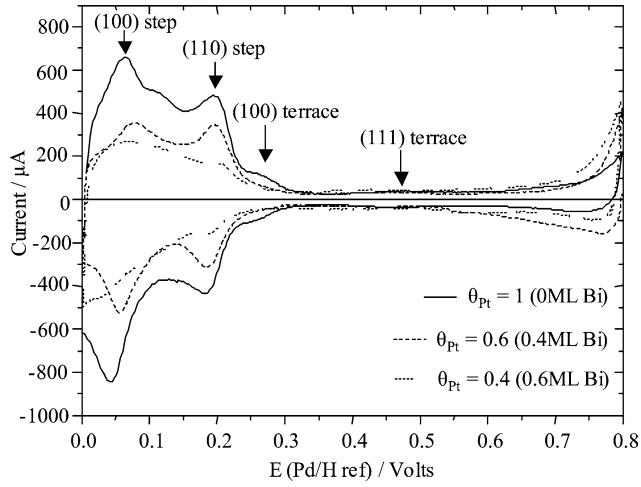

Fig. 7. Cyclic voltammograms for Bi-modified and unmodified catalysts.

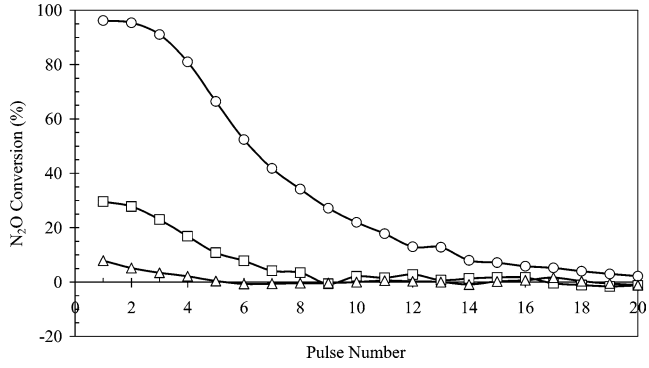

Fig. 8. Conversion of N_2O as a function of pulse number with Bi modified and unmodified catalysts. Total gas flow = 50 $cm^3\,min^{-1}$, pulses of 2000 ppm N_2O, He balance. 5% Pt/C (○), 0.4 ML Bi/Pt/C (□), 0.6 ML Bi/Pt/C (△). Pretreatment: 1% H_2/He, 120 °C. Pulsing performed at 2 °C.

and 0.35 V and (111)-broad peak centered at 0.47 V) this appeared to have relatively short range order [54]. This catalyst also exhibited a fairly high number of defect sites (kinks) as signified by the broadness of the defect peaks relative to the much sharper peaks observed for single crystals containing linear steps [55]. The 0.4 ML Bi/Pt catalyst, in accordance with the known adsorption behavior of Bi on Pt (i.e., kinks blocked before steps [56]), showed a partial blockage of the (100) and (110) defect sites. (100) terraces were also slightly affected but (111) terrace density remained virtually unchanged. The 0.6 ML Bi/Pt catalyst showed continued adsorption of Bi at both step sites (all defect peak intensity has been lost) while coverage at terrace sites remained virtually unchanged from the previous sample. The onset of bismuth adsorption on (111) terraces is signified by the appearance of a characteristic surface redox peak at 0.55 V [33], which was not observed for the catalyst samples used here.

Fig. 8 shows the results of N_2O pulse experiments with the Pt/C and Bi/Pt/C catalysts. From this plot it can be seen that addition of the bismuth had a significant effect on the conversion of N_2O per pulse. The Pt/C base catalyst exhibited > 90% N_2O conversion activity for 3 pulses, before

the conversion decreased. The 0.4 ML Bi/Pt/C catalyst converted 30% of the first 2–3 N_2O pulses before deactivation occurred. As stated previously, this catalyst had partially blocked defect sites, while the terraces remained open. N_2O conversion decreased as a result of blocking of defect sites with Bi, which indicated that defect sites were active for N_2O decomposition. The 0.6 ML Bi/Pt/C catalyst decomposed even less N_2O, suggesting that the Bi had blocked the majority of the active sites required for N_2O decomposition. Complete blockage of the defects by Bi had occurred, while the terraces ((111) and (100)) remained open. The limited conversion of N_2O at these sites suggested that terraces have a low activity for N_2O decomposition. The limited nature of the conversion may be due to the fact that the number of terrace sites were themselves limited, or that the rate of decomposition on terraces was less than at defects.

This apparent difference in the rate of reaction on defect as compared with terrace surfaces needs to be rationalized with respect to the DFT results presented previously. Because the N_2O chemisorption on Pt is weak, the N_2O dissociation is not likely to occur through a precursor-mediated mechanism. In other words, N_2O molecules may directly dissociate on the surface from the gas phase. Then the degree of molecule distortion at the transition state is very important in determining the probability for molecules to overcome the activation barrier. It is expected that the higher the degree of distortion of the N_2O molecules, the lower the probability of dissociation. The degree of molecular bending by N_2O on the (211) surface is significantly less (N–N–O bond angle: 137°) relative to the structure of the transition state on Pt(111) (N–N–O bond angle: 120°). This suggests that the structure of the transition state at the stepped (211) surface has a higher probability of occurring than the more strained structure observed on Pt(111).

The temperature of the catalyst pretreatment was also a critical factor in these experiments. Bi will thermally desorb from a Pt surface over the temperature range 400–1000 °C [57]. However, it must be considered to be mobile on the surface at slightly lower temperatures. Fig. 9 illustrates the results of N_2O decomposition with the two Bi/Pt catalysts under different pretreatment conditions. At 120 °C, the 0.4 ML Bi catalyst decomposed N_2O in considerable amounts before deactivation by $O_{(ads)}$ accumulation. However, with a pretreatment temperature of 300 °C, ∼ 20% of the first pulse was converted before rapid deactivation of the catalyst occurred. Pretreatment of the 0.6 ML Bi catalyst at 300 °C completely deactivated the catalyst, with no decomposition of N_2O occurring. Since Bi melts at 271 °C [58], these results suggest that, upon heating to 300 °C, significant and irreversible changes to the catalyst occurred, perhaps even alloying of the bismuth and platinum. At 120 °C, the catalyst is reduced with no measurable change in the distribution of Bi adatoms. Indeed, Fig. 10 shows the cyclic voltammetry analysis results of the effects of the different temperature pretreatments. It is clear from the figure that the temperature of the pretreatment significantly alters the state

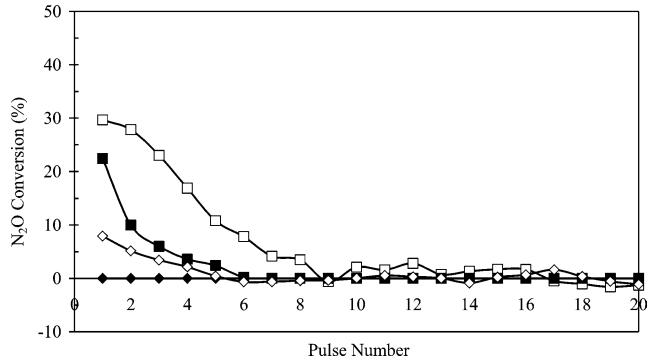

Fig. 9. The effect of pretreatment temperature on the conversion of N_2O as a function of pulse number with Bi modified and unmodified catalysts. Total gas flow = 50 $cm^3\ min^{-1}$, pulses of 2000 ppm N_2O, He balance. 0.4 ML Bi/Pt/C (□), 0.6 ML Bi/Pt/C (◇). Open symbols refer to a pretreatment at 120 °C, the closed symbols refer to a pretreatment at 300 °C. Pulsing of N_2O was always at room temperature.

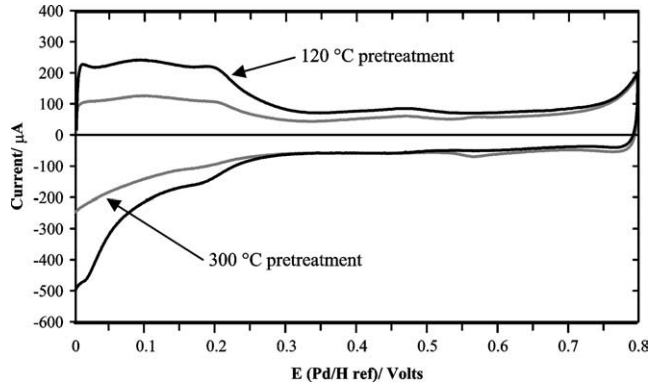

Fig. 10. Cyclic voltammograms for 0.4 ML Bi/Pt/C catalyst pretreated at 120 °C (black) and 300 °C (gray) (1% H_2/He, 30 min, TF 50 $cm^3\ min^{-1}$).

of the catalyst. A pretreatment of 120 °C for the 0.4 ML Bi catalyst shows that responses for the stepped surfaces ((110)-peak at 0.05–0.1 V and the (111)-peak at 0.2 V) are approximately the same as displayed in Fig. 7. In addition, the (111) terrace density (broad peak centered at 0.5 V) remains virtually unchanged from the original sample shown in Fig. 7. However, pretreatment of the catalyst at 300 °C significantly reduces the density for all these surfaces. This indicates that some Bi/Pt alloying may have occurred. Similar changes for the 0.6 ML Bi catalyst were observed to occur as a result of the pretreatment temperature (results not shown).

We previously reported that N_2O decomposition was favored to occur at defect sites [59]. Those studies were performed with a pretreatment temperature of 300 °C which we now know can result in alloy formation. However, the overall conclusions are validated by the present experiments with bismuth-modified catalysts activated at 120 °C.

It is clear that in pulse experiments, with a short contact time, blocking of defect sites lowers the activity for N_2O dissociation. On the other hand, the DFT calculations indicate that N_2O decomposition may occur on both stepped and flat platinum surfaces at temperatures as low as 25 °C. This is

in contrast to NO dissociation, which is significantly more facile at defect sites [48,60–66].

The apparent discrepancy between the experimental results (edges more active than terraces under pulse conditions) and the DFT calculations (similar barriers on edges and terraces) can be rationalized as follows. Although DFT calculations show that the barrier of N_2O dissociation on Pt(111) is similar to that on Pt(211), the probability of achieving the transition state on Pt(111) should be much smaller because a larger distortion is required. Therefore, the absolute reaction rate on the flat surfaces should be much smaller than that on defects.

4. Conclusions

Both DFT calculations and pulsed N_2O experiments show that reduced platinum could be active toward N_2O decomposition at temperatures as low as 25 °C. However, the strong Pt–O bond means that the active sites are rapidly poisoned by $O_{(ads)}$. The DFT calculations show that both step (211) and terrace (111) sites have low barriers for N_2O dissociation of 0.44 and 0.32 eV, respectively. However, the structure at the transition state on Pt(111) involves a significantly greater distortion of the N–N–O molecular bond angle, thereby suggesting that the preexponential factors would be much smaller so the rate of decomposition would be less on this surface. Controlled, irreversible adsorption of inactive bismuth to Pt/C catalysts preferentially blocked defect sites before terraces sites. Complete blockage of the defect sites significantly decreases the conversion of N_2O. The terrace sites remained unaffected by Bi addition and a small amount of N_2O conversion was still observed, suggesting both surfaces are active for N_2O decomposition but that defect sites have a much higher activity under pulsing conditions, as was indicated by the DFT results.

In conclusion, this combination of experimental and theoretical work has provided both additional insight into the nature of the N_2O dissociation on Pt catalysts and a valuable reality check on DFT calculations for supported catalysts. The use of bismuth modification to block specific sites on Pt so that the rate of N_2O dissociation on different surfaces can be determined directly is a useful technique. The apparent discrepancy between the calculated activation barriers and the experimental rates draws attention to the importance of linking experiment and theory to avoid possible misinterpretation of the results of DFT calculations.

Acknowledgments

S.D. thanks DHFETE for funding. We are grateful to Prof. G. Attard, Mr. D.J. Jenkins, and Mr. M. Greenslade for providing the bismuth-modified catalysts and the corresponding CV results. The Super-Computing Centre in Ireland and the HP SuperComputer at QUB are acknowledged for computing time. We are thankful for the many useful discussions with Dr. M.D. Coleman.

References

[1] J. Kaspar, P. Fornasiero, N. Hickey, Catal. Today 77 (2003) 419.
[2] A. Fritz, V. Pitchon, Appl. Catal. B 13 (1997) 1.
[3] R. Burch, M.D. Coleman, J. Catal. 208 (2002) 435.
[4] G. Centi, A. Galli, B. Montanari, S. Perathoner, A. Vaccari, Catal. Today 35 (1997) 113.
[5] G. Centi, L. Dall'Olio, S. Perathoner, J. Catal. 192 (2000) 224.
[6] G. Centi, L. Dall'Olio, S. Perathoner, Appl. Catal. A 194–195 (2000) 79.
[7] F. Kapteijn, J. Rodriguez-Mirasol, J.A. Moulijn, Appl. Catal. B 9 (1996) 25.
[8] E.R.S. Winter, J. Catal. 15 (1969) 144.
[9] E.R.S. Winter, J. Catal. 19 (1970) 32.
[10] E.R.S. Winter, J. Catal. 34 (1974) 431.
[11] W.H. Weinberg, J. Catal. 28 (1973) 459.
[12] N.R. Avery, Surf. Sci. 131 (1983) 501.
[13] C.G. Takoudis, L.D. Schmidt, J. Catal. 80 (1983) 274.
[14] H.G. Lintz, L. Riekert, J. Catal. 88 (1984) 244.
[15] M.H. Kim, J.R. Ebner, R.M. Friedman, M.A. Vannice, J. Catal. 204 (2001) 348.
[16] P. Denton, Y. Schuurman, A. Giroir-Fendler, H. Praliaud, M. Primet, C. Mirodatos, C. R. Acad. Sci. Paris, Ser. IIc, Chem. 3 (2000) 437.
[17] R. Burch, P.J. Millington, A.P. Walker, Appl. Catal. B 4 (1994) 65.
[18] A. Obuchi, A. Ogata, H. Takahashi, J. Oi, G.R. Bamwenda, K. Mizuno, Catal. Today 29 (1996) 103.
[19] J. Oi, A. Obuchi, G.R. Bamwenda, A. Ogata, H. Yagita, S. Kushiyama, K. Mizuno, Appl. Catal. B 12 (1997) 277.
[20] G.R. Bamwenda, A. Obuchi, A. Ogata, J. Oi, S. Kushiyama, K. Mizuno, J. Mol. Catal. A: Chem. 126 (1997) 151.
[21] B.K. Cho, J. Catal. 148 (1994) 697.
[22] B.K. Cho, J. Catal. 162 (1996) 149.
[23] B.K. Cho, J. Catal. 138 (1992) 255.
[24] Y. Ohno, K. Kimura, M. Bi, T. Matsushima, J. Chem. Phys. 110 (1999) 8221.
[25] Y. Ohno, I. Kobal, H. Horino, I. Rzeznicka, T. Matsushima, Appl. Surf. Sci. 169–170 (2001) 273.
[26] R. Burch, A.A. Shestov, J.A. Sullivan, J. Catal. 188 (1999) 69.
[27] R. Burch, A.A. Shestov, J.A. Sullivan, J. Catal. 182 (1999) 497.
[28] R. Burch, A.A. Shestov, J.A. Sullivan, J. Catal. 186 (1999) 353.
[29] R. Burch, J.A. Sullivan, J. Catal. 182 (1999) 489.
[30] A.A. Shestov, R. Burch, J.A. Sullivan, J. Catal. 186 (1999) 362.
[31] A.A. Shestov, R. Burch, J.A. Sullivan, React. Kinet. Dev. Catal. Process. (1999) 455.
[32] K. Rahkamaa, T. Salmi, Chem. Eng. Sci. 54 (1999) 4343.
[33] R.W. Evans, G.A. Attard, J. Electroanal. Chem. 345 (1992) 337.
[34] M.C. Payne, M.P. Teter, D.C. Allen, T.A. Arias, J.D. Joannopolous, Rev. Mod. Phys. 64 (1992) 1045.
[35] P. Hu, D.A. King, M.H. Lee, M.C. Payne, Chem. Phys. Lett. 246 (1995) 73.
[36] P. Hu, D.A. King, S. Crampin, M.H. Lee, M.C. Payne, Chem. Phys. Lett. 230 (1994) 501.
[37] J.P. Perdew, J.A. Chevary, S.H. Vosko, K.A. Jackson, M.R. Pederson, D.J. Singh, C. Fiolhais, Phys. Rev. B 46 (1992) 6671.
[38] D. Vanderbilt, Phys. Rev. B 41 (1990) 7892.
[39] A. Alavi, P. Hu, T. Deutsch, P.L. Silvestrelli, J. Hutter, Phys. Rev. Lett. 80 (1998) 3650.
[40] C.J. Zhang, P. Hu, J. Am. Chem. Soc. 122 (2000) 2134.
[41] C.J. Zhang, P. Hu, J. Am. Chem. Soc. 123 (2001) 1166;
A. Michaelides, P. Hu, J. Am. Chem. Soc. 122 (2000) 9866.
[42] S. Tanaka, K. Yuzaki, S. Ito, S. Kameoka, K. Kunimori, J. Catal. 200 (2001) 203.

[43] Y. Li, M. Bowker, Surf. Sci. 348 (1996) 67.
[44] Z.-P. Liu, P. Hu, J. Chem. Phys. 114 (2001) 8244.
[45] J.K. Norskov, T. Bligaard, A. Logdottir, S. Bahn, L.B. Hansen, M. Bollinger, H. Bengaard, B. Hammer, Z. Sljivancanin, M. Mavrikakis, Y. Xu, S. Dahl, C.J.H. Jacobsen, J. Catal. 209 (2002) 275.
[46] A. Bogicevic, K.C. Hass, Surf. Sci. Lett. 506 (2002) L237.
[47] K. Bleakley, P. Hu, J. Am. Chem. Soc. 121 (1999) 7644.
[48] C.J. Zhang, P. Hu, M.-H. Lee, Surf. Sci. 432 (1999) 305.
[49] J.J. Mortensen, B. Hammer, J.K. Norskov, Surf. Sci. 414 (1998) 315.
[50] S. Tanaka, K. Yuzaki, S. Ito, H. Uetsuka, S. Kameoka, K. Kunimori, Catal. Today 63 (2000) 413.
[51] J. Leglise, J.O. Petunchi, W.K. Hall, J. Catal. 86 (1984) 392.
[52] K. Yuzaki, T. Yarimizu, S.-I. Ito, K. Kunimori, Catal. Lett. 47 (1997) 173.
[53] K. Yuzaki, T. Yarimizu, K. Aoyagi, S. Ito, K. Kunimori, Catal. Today 45 (1998) 129.
[54] A. Wieckowski, Interfacial Electrochemistry, Dekker, New York, 1999.
[55] J. Clavilier, K. El-Achi, A. Rodes, Chem. Phys. 141 (1990) 1.
[56] G.A. Attard, A. Ahmadi, D.J. Jenkins, O. Hazzai, P.B. Wells, K.G. Griffin, P. Johnston, J.E. Gillies, submitted for publication.
[57] M.T. Paffett, C.T. Campbell, T.N. Taylor, J. Chem. Phys. 85 (1986) 6176.
[58] D.R. Lide, Handbook of Chemistry and Physics, CRC Press, Boca Raton, FL, 2002–2003.
[59] R. Burch, G.A. Attard, S.T. Daniells, D.J. Jenkins, J.P. Breen, P. Hu, Chem. Commun. (2002) 2738.
[60] B. Hammer, J. Catal. 199 (2001) 171.
[61] L. Olsson, V.P. Zhdanov, B. Kasemo, Surf. Sci. 529 (2003) 338.
[62] R.I. Masel, Catal. Rev. Sci. Eng. 28 (1986) 335.
[63] C.T. Campbell, G. Ertl, J. Segner, Surf. Sci. 115 (1982) 309.
[64] R.J. Gorte, L.D. Schmidt, J.L. Gland, Surf. Sci. 109 (1981) 367.
[65] S.B. Lee, D.H. Kang, C.Y. Park, H.T. Kwak, Bull. Korean Chem. Soc. 16 (1995) 157.
[66] M. Haneda, Y. Kintaichi, I. Nakamura, T. Fujitani, H. Hamada, Chem. Commun. (2002) 2816.